Modified surface plasmonic waveguide formed by nanometric parallel lines*

Xue Wen-Rui(薛文瑞)†, Guo Ya-Nan(郭亚楠), and Zhang Wen-Mei(张文梅)

College of Physics and Electronic Engineering, Shanxi University, Taiyuan 030006*, China*

(Received 20 March 2009; revised manuscript received 29 June 2009)

In this paper, two kinds of modified surface plasmonic waveguides formed by nanometric parallel lines are proposed. The finite-difference frequency-domain method is used to study propagation properties of the fundamental mode supported by these surface plasmonic waveguide structures. Results show that the transverse magnetic field of the fundamental mode is mainly distributed in the face to face region formed by two rods. With the same geometrical parameters and the same working wavelength of 632.8 nm, in the case of rods with a triangular cross-section, the degree of localization of field is strong, i.e. the mode area is small, but the fraction of the modal power in the metal increases, so the effective index increases and the propagation length of the mode decreases. With the same geometrical parameters, relative to the case of a working wavelength of 632.8 nm, when working wavelength is large, the mode area of transverse magnetic field distribution is large, i.e. the degree of localization of field is weak, and the interaction of field and silver is weak too, then the effective index decreases, so the propagation length increases. The rounded radii of rods have a great influence on the performance of the surface plasmonic waveguides with rounded triangular cross-sections, but have little influence on the performance of surface plasmonic waveguides with rounded square cross-sections. Since the distribution of transverse magnetic field, effective index, propagation length and the mode area can be adjusted by the geometrical parameters, this kind of modified surface plasmonic waveguide can be applied to the field of photonic device integration and sensors.

Keywords: surface plasmon polaritons, optical waveguides

PACC: 7320M, 4280L

1. Introduction

The interaction of light with matter in nanostructured metallic structures has led to a new branch of photonics called plasmonics. Surface plasmonic waveguides (SPWs) are basic devices in plasmonics. Along the surface of metals, such waveguides guide light in the form of surface plasmon polaritons (SPPs) with lateral dimensions on the order of subwavelength. Because this kind of waveguide is compatible with existing fabrication technologies, it is believed that these waveguides can be used to overcome the diffraction limit, to offer the possibility of integration of electronics and photonics on the same chip and to fulfil the further miniaturization of photonic devices and high integration density of photonic chips.[1−4]

By now, many SPWs have been studied theoretically and experimentally.[5−25] Because wedge SPWs[17,20] can provide relatively long propagation length as well as a strong mode confinement, they have attracted much attention. As suggested by Takahara *et al.*,[5] one can construct a kind of SPW by embedding nanometric parallel lines with circular cross sections in dielectric background. This kind of SPW can be regarded as a combination of two wedge SPWs. Can the cross section of the parallel lines be changed to another wedged one, for example, a triangular or square cross section? What are the influences on their performance with different cross sections of the parallel lines? Up to now, these questions have not been analysed yet and are still open.

In this paper, two kinds of modified SPWs formed by nanometric parallel lines are studied. The finite-difference frequency-domain (FDFD) method[26−28] is used to study their propagation properties. Distribution of transverse magnetic field intensity, effective index, propagation length and mode area of the fundamental mode with longer propagation length supported by these SPW structures will be discussed.

2. Structure and simulation method

The cross sections of the proposed SPWs formed by nanometric parallel lines in this paper are shown in Figs. 1(a) and 1(b). The first SPW is composed of two

*Project supported by the National Natural Science Foundation of China (Grant No. 60771052) and the Natural Science Foundation of Shanxi Province, China (Grant No. 2006011029).

†Corresponding author. E-mail: wrxue@sxu.edu.cn

© 2010 Chinese Physical Society and IOP Publishing Ltd

metal rods with a rounded triangular cross section. The second SPW is composed of two metal rods with a rounded square cross section. For comparison, the third SPW which is composed of two metal rods with a circular cross section, proposed by Takahara *et al.*,[5] is shown in Fig. 1(c). These metal rods are all embedded in dielectric background. In Figs. 1(a), 1(b) and 1(c), $2c$ is the centric distance of the two rods, a is the radius or the distance from the centre to the vertex of the rod, r is the rounded radius of the rod; $\varepsilon_{\rm m}$ is the dielectric constant of metal rods, and $\varepsilon_{\rm clad}$ is the dielectric constant of the background. In the calculation, the primary material is chosen to be silver and the dielectric constant $\varepsilon_{\rm m}$ is chosen to be –14.8817 + 0.3858j (λ = 548.7 nm), –18.0550 + 0.4776j (λ = 632.8 nm), and –31.0784 + 0.4118j (λ = 800.0 nm).[29] To support the nanometric parallel lines, the background material is chosen to be SiO_2, and its dielectric constant $\varepsilon_{\rm clad}$ is 2.0736. Because the value of $\varepsilon_{\rm clad}$ is real and about one order smaller than the real part of $\varepsilon_{\rm m}$, we neglected its dispersion here.

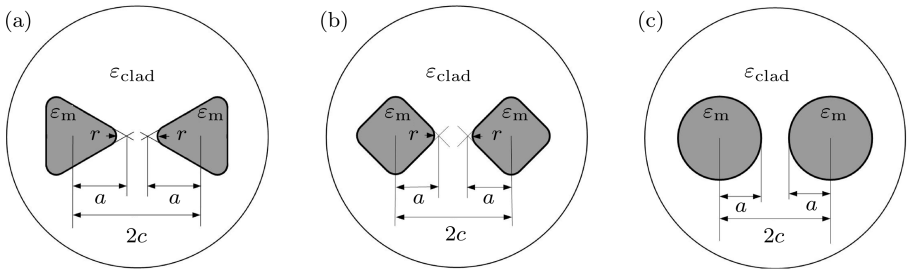


Fig. 1. Cross sections of the surface plasmonic waveguides formed by (a) triangular, (b) square and (c) circular[5] nanometric parallel lines. Here, $2c$ is the centric distance of the two rods, a is the radius or the distance from the centre to the vertex of the rod, r is the rounded radius of the rod. $\varepsilon_{\rm m}$ is the dielectric constant of metal rods, and $\varepsilon_{\rm clad}$ is the dielectric constant of the background.

In this paper, the 2D full-vectorial FDFD method[26–28] is used to study the propagation properties of the SPW structures. Given the geometrical parameter, electromagnetic parameter and working wavelength, the propagation constant, effective index and the distribution of magnetic field of each mode at the working wavelength can be obtained by solving the eigenvalue equation using Arnoldi arithmetic.[30] 601×601 lattices are adopted to discretize the whole computational domain, and 20 layers of them are perfectly matched layer absorbing boundary layers (APML) that are used to truncate the lattices. The spatial discretization distance is $\Delta x = \Delta y = 1.0$ nm. The accuracy of the FDFD code adopted in this paper has been validated in our previous work.[22–24]

3. Results and discussions

Mode characteristics of the surface plasmonic waveguide with three kinds of cross sections shown in Fig. 1 are investigated first. It is found that there are many modes that can be supported by these kinds of SPWs, but the fundamental mode is more suitable for guiding electromagnetic waves. The distribution of transverse magnetic field intensity $|H_t|^2$ of the fundamental mode, in the case of $a = 75$ nm, $c = 103$ nm, $r = 5$ nm and $\lambda = 632.8$ nm, is shown in Figs. 2(a), 2(b), and 2(c). Here the transverse magnetic field intensity is defined as $|H_t|^2 = H_x^2 + H_y^2$; H_x and H_y are components of the magnetic field.

It can be seen from Figs. 2(a), 2(b), and 2(c) that the transverse magnetic field of the fundamental mode is mainly distributed in the face to face region which is formed by two rods. In the three cases of rods with triangular, square and circular cross sections when $a = 75$ nm, $c = 103$ nm, $r = 5$ nm and $\lambda = 632.8$ nm, the two corner angles are smallest and the two corner tips are sharpest in the case of rods with triangular cross section, so the degree of localization of field is the largest.

Since effective index $\mathrm{Re}(n_{\rm eff})$, propagation length $L_{\rm prop}$ and mode area $A_{\rm m}$ are the three most important physical quantities that describe the propagation properties of SPWs, we next investigate the dependence of $\mathrm{Re}(n_{\rm eff})$, $L_{\rm prop}$ and $A_{\rm m}$ of the modes shown

in Fig. 2 on the geometrical parameter c. Here $\mathrm{Re}(n_{\mathrm{eff}})$ is defined as $\mathrm{Re}(\beta)\lambda/2\pi$, L_{prop} defined as $L_{\mathrm{prop}} = 1/\mathrm{Im}(\beta)$, and the A_{m} defined as the occupied area of the transverse magnetic field intensity $|H_t|^2$ when its altitude decreases from 100% to 10%.

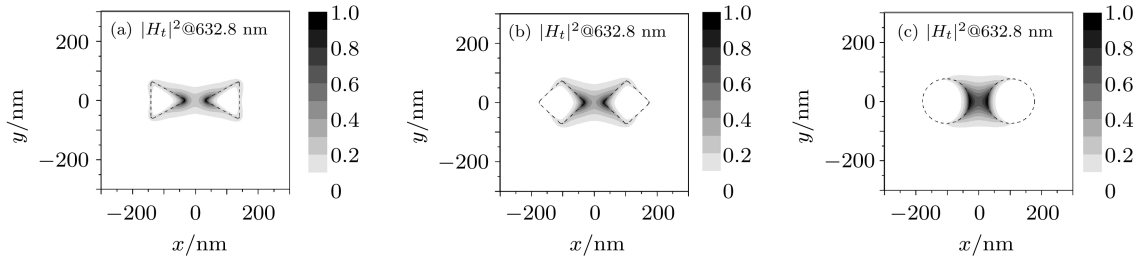


Fig. 2. Distribution of transverse magnetic field intensity of the SPWs with (a) rounded triangular cross section, (b) rounded square cross section and (c) circular cross section for $a = 75$ nm, $c = 103$ nm and $r = 5$ nm at $\lambda = 632.8$ nm.

The variations of $\mathrm{Re}(n_{\mathrm{eff}})$, L_{prop} and A_{m} with c in the three cases of $a = 50$, 75 and 100 nm are shown in Figs. 3(a), 3(b), and 3(c) respectively. It can be seen from these figures that curves can be obviously separated into three groups according to different a. In each group, $\mathrm{Re}(n_{\mathrm{eff}})$ decreases as c increases; however, L_{prop} and A_{m} increase as c increases. The position of curves in each group is influenced by the cross section of rods. We also find that there is a trade-off between the degree of localization of field and the propagation length.[1] In the case of rods with triangular cross section, the degree of localization of field is strong, i.e. the mode area is small, but the fraction of the modal power in the metal increases, the effective index increases and the propagation length of the mode decreases. In the case of rods with circular cross section, the degree of localization of field is weak, i.e. the mode area is large, but the fraction of the modal power in the metal decreases, the effective index decreases and the propagation length of the mode increases.

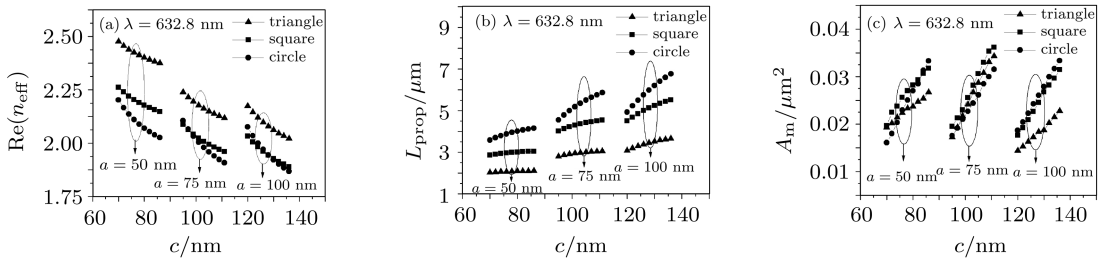


Fig. 3. Dependence of (a) effective index, (b) propagation length and (c) mode area of different SPWs on c when $r = 5$ nm and $\lambda = 632.8$ nm.

Thirdly, in order to find out the dependence of transverse magnetic field distribution of the modes shown in Fig. 2 on the working wavelength, the field intensity distributions for different cross sections of rods with $a = 75$ nm, $c = 103$ nm and $r = 5$ nm at $\lambda = 800.0$ nm and 548.7 nm are calculated respectively. Here we extend the calculation to a longer wavelength, 800 nm, where vertical-cavity surface-emitting lasers (VCSELs) are available. The results obtained are shown in Fig. 4.

It can be seen from Fig. 4 that the transverse magnetic field distribution is similar to that in Fig. 2. Compared with the case of Figs. 2(a), 2(b), and 2(c), in the case of Figs. 4(a), 4(c), and 4(e), the mode area of transverse magnetic field distribution becomes larger. However, in the case of Figs. 4(b), 4(d), and 4(f), the mode area of transverse magnetic field distribution becomes smaller.

Figures 5(a)–5(c), 5(d)–5(f) and 5(g)–5(i) also show the dependences of $\mathrm{Re}(n_{\mathrm{eff}})$, L_{prop} and A_{m} on c for $a = 75$ nm, $r = 5$ nm, $\lambda = 548.7$ nm, 632.8 nm and 800.0 nm. It can be seen that the curves of $\mathrm{Re}(n_{\mathrm{eff}})$, L_{prop} and A_{m} could also be separated into three groups according to different cross sections. In each group, $\mathrm{Re}(n_{\mathrm{eff}})$ decreases with the increase of c; however, L_{prop} and A_{m} increase with the increase of c.

The working wavelength has a great influence on the position of the curves in these figures. We can also see from Figs. 5(d)–5(f) that curves for $\lambda = 800.0$ nm are always at the uppermost of each group of curves. This phenomenon can be explained by the different transverse magnetic field distributions at different wavelengths. Compared to the case of $\lambda = 632.8$ nm, when λ is smaller, the mode area of transverse magnetic field distribution is small, i.e. the degree of localization of field is strong, and the interaction of field and silver is strong too, then the effective index increases, and so the propagation length decreases. However, when λ is larger, the mode area of transverse magnetic field distribution is larger, i.e. the degree of localization of field is weak, and the interaction of field and silver is weak too, then the effective index decreases, and so the propagation length increases.

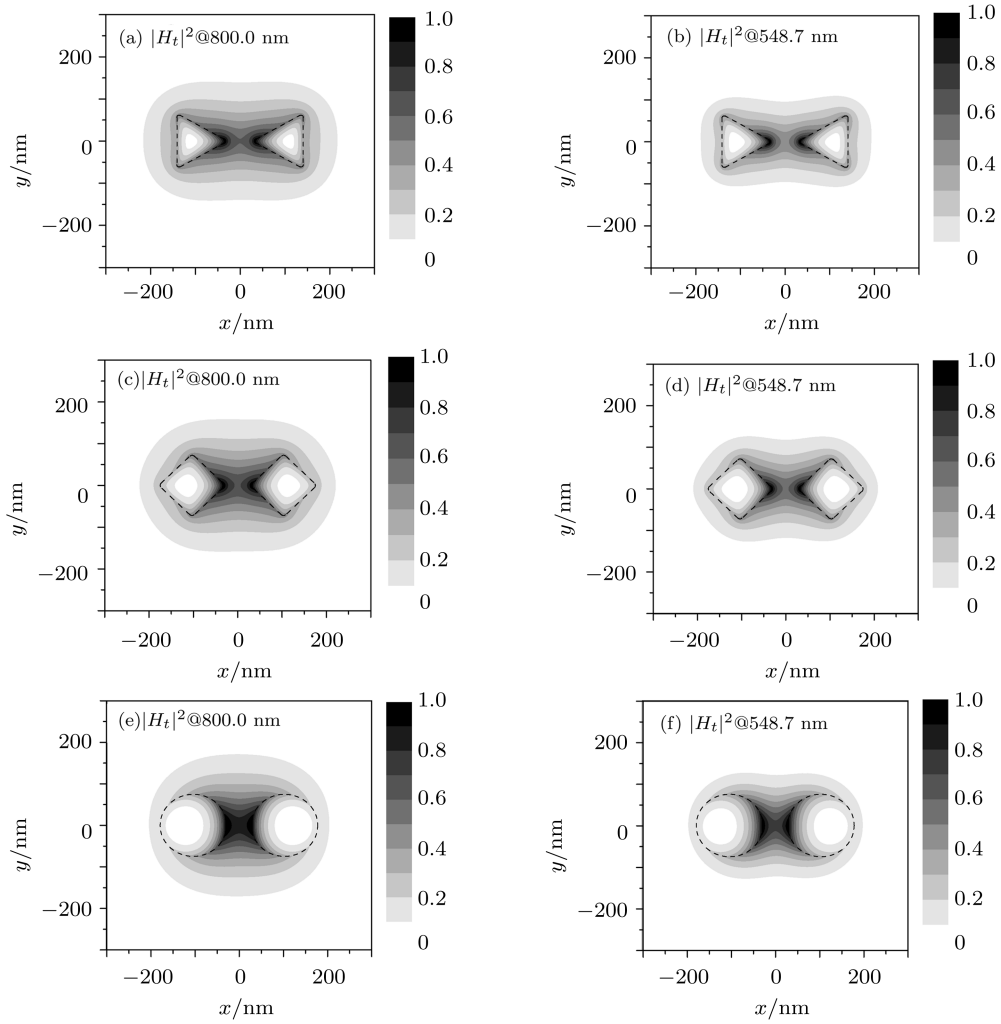


Fig. 4. Distributions of transverse magnetic field intensity of the SPWs for (a) and (b) rounded triangular cross section, (c) and (d) rounded square cross section, and (e) and (f) circular cross section when $a = 75$ nm, $c = 103$ nm and $r = 5$ nm at $\lambda = 800.0$ nm and 548.7 nm.

Finally, let us investigate the dependence of the distribution of transverse magnetic field intensity, effective index, propagation length and mode area of the proposed SPWs on the rounded radius r.

Distributions of transverse magnetic field intensity of SPWs with rounded triangular cross section and with rounded square cross section, for $a = 100$ nm, $c = 128$ nm, $r = 5$ nm or 10 nm and $\lambda = 632.8$ nm, are shown in Fig. 6. It can be seen that the transverse magnetic field distribution of SPWs with the same cross section is similar to each other. Compared to the case of $r = 5$ nm (Figs. 6(a) and 6(c)), in the case of $r = 10$ nm (Figs. 6(b) and 6(d)), the mode area of transverse magnetic field distribution increases slightly.

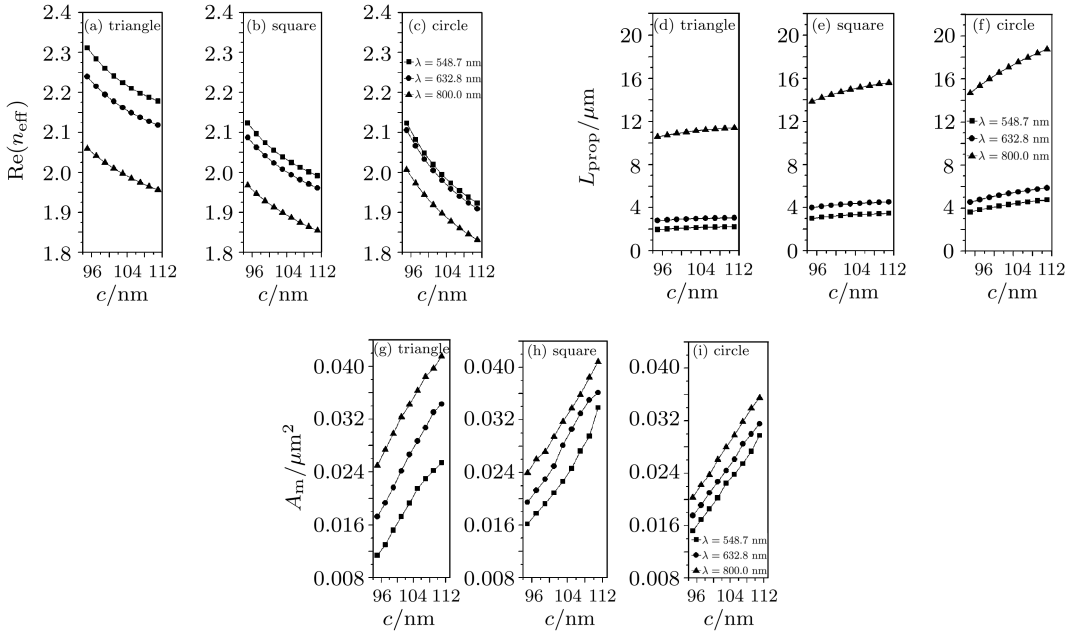


Fig. 5. Dependence of effective index (a)–(c), propagation length (d)–(f) and mode area (g)–(i) of different SPWs on c for $a = 75$ nm, $r = 5$ nm, $\lambda = 548.7$ nm, 632.8 nm and 800.0 nm.

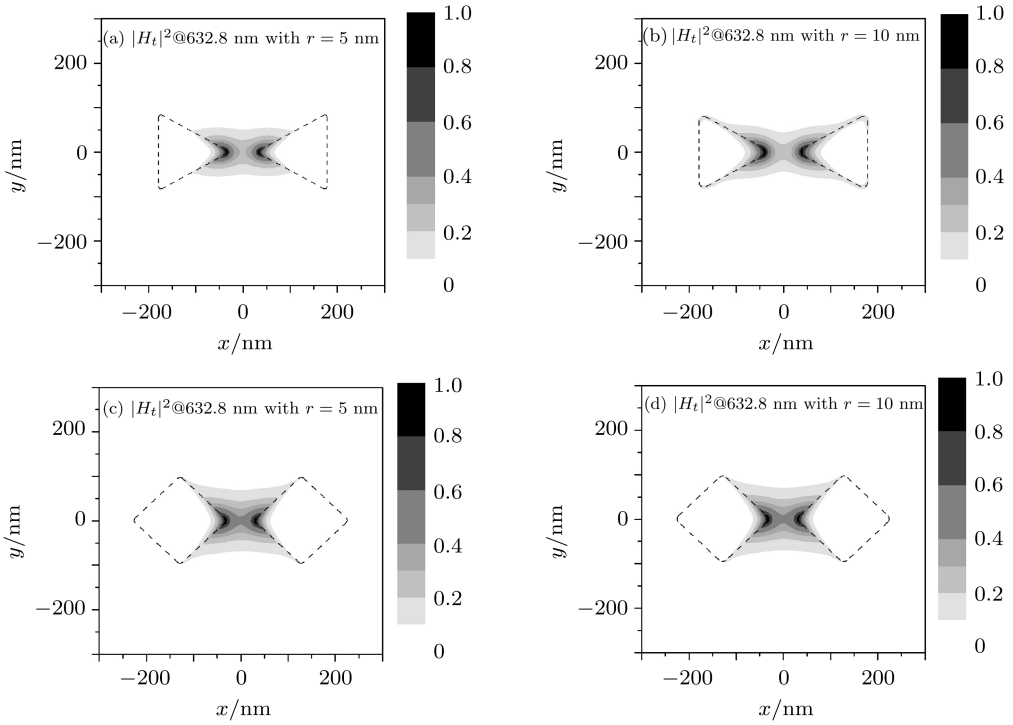


Fig. 6. Distributions of transverse magnetic field intensity of the SPWs with rounded triangular cross section (a) and (b), rounded square cross-section (c) and (d) when $a = 100$ nm, $c = 128$ nm, $r = 5$ nm or 10 nm and $\lambda = 632.8$ nm.

Dependence of effective index, propagation length and mode area of SPWs with rounded triangular cross section and with rounded square cross section on c, for the case of $a = 100$ nm, $r = 5$ nm or 10 nm and $\lambda = 632.8$ nm, is shown in Fig. 7. For comparison, curves corresponding to the SPW with circular cross section and $a = 100$ nm are shown also in Fig. 7. It can be seen that the curves could be separated into three groups according to the cross section. In each group, when c increases, effective index decreases, but propagation length and mode area increase. The curve corresponding to the SPW with $r = 10$ nm takes on a smaller effective index, but larger propagation length and mode area.

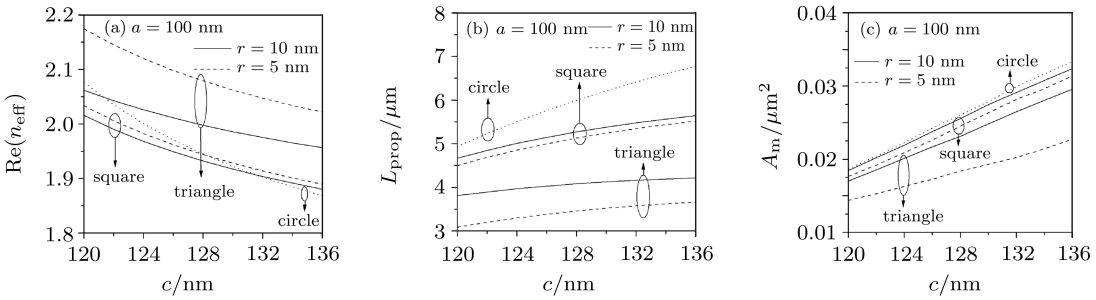


Fig. 7. Dependence of effective index (a), propagation length (b) and mode area (c) of different SPWs on c when $a = 100$ nm, $\lambda = 632.8$ nm, $r = 5$ nm and 10 nm.

From Figs. 6 and 7, one can find that the rounded radius r has a great influence on propagation properties of the SPW with rounded triangular cross section, but has little influence on the propagation properties of the SPW with rounded square cross section. This phenomenon can be explained by the coupling intensity of the SPPs propagating along the nanometric parallel lines. Because the corner angle of the unrounded triangular cross section is smaller than that of the unrounded squre cross section, the tip of the former is sharper than the latter. When the face to face tip of the nanometric parallel lines are rounded, the change of coupling intensity of the SPPs propagating along the nanometric parallel lines in the case of triangular cross section is larger than that in the case of square cross section, so the rounded radius r has a great influence on the propagation properties of the SPW with rounded triangular cross section than on that with rounded square cross section.

4. Conclusion

In this paper, we have designed two modified surface plasmonic waveguides formed by nanometric parallel lines. The numerical calculations show:

(i) The transverse magnetic field of the fundamental mode is mainly distributed in the face to face region formed by two rods. This mode is suitable for guiding electromagnetic waves.

(ii) With the same geometrical parameters at $\lambda = 632.8$ nm, in the case of rods with triangular cross section, the degree of localization of field is strong, i.e. the mode area is small, but the fraction of the modal power in the metal increases, the effective index increases, and the propagation length of the mode decreases.

(iii) With the same geometrical parameters, as compared with the case of $\lambda = 632.8$ nm, when λ is small, the mode area of transverse magnetic field distribution is small, i.e. the degree of localization of field is strong, and the interaction of field and silver is strong too, then the effective index increases, and so the propagation length decreases. However, when λ is large, the mode area of transverse magnetic field distribution is large, i.e. the degree of localization of field is weak, and the interaction of field and silver is weak too, then the effective index decreases, and so the propagation length increases.

(iv) The rounded radius r has a great influence on the propagation properties of the SPW with rounded triangular cross section, but has little influence on those of the SPW with rounded square cross section.

Since distribution of transverse magnetic field, effective index, propagation length and the mode area can be adjusted by the geometrical parameters, this kind of modified SPW can be applied to the field of photonic device integration and sensors.

References

[1] Barnes W L, Dereux A and Ebbesen T W 2003 *Nature* **424** 824

[2] Ozbay E 2006 *Science* **311** 189

[3] Bozhevolnyi S I, Volkov V S, Devaux E, Laluet J Y and Ebbesen T W 2006 *Nature* **440** 508

[4] Maier S A 2006 *IEEE J. Sel. Top. Quant.* **12** 1671

[5] Takahara J, Yamagishi S, Taki H, Morimoto A and Kobayashi T 1997 *Opt. Lett.* **22** 475

[6] Berini P 1999 *Opt. Lett.* **24** 1011

[7] Maier S A, Kik P G, Atwater H A, Meltzer S, Harel E, Koel B E and Requicha A G 2003 *Nat. Mater.* **2** 229
[8] Pile D F P and Gramotnev D K 2004 *Opt. Lett.* **29** 1069
[9] Wang B and Wang G P 2004 *Appl. Phys. Lett.* **85** 3599
[10] Pile D F P, Ogawa T, Gramotnev D K, Matsuzaki Y, Vermon K C, Yamaguchi K, Okamoto T, Haraguchi M and Fukui M 2005 *Appl. Phys. Lett.* **87** 261114
[11] Liu L, Han Z and He S 2005 *Opt. Express* **13** 6645
[12] Wang G P and Wang B 2006 *J. Opt. Soc. Am.* B **23** 1660
[13] Chen L, Wang B and Wang G P 2006 *Appl. Phys. Lett.* **89** 243120
[14] Jung J, Sondergaard T and Bozhevolnyi S I 2007 *Phys. Rev.* B **76** 035434
[15] Lee I, Jung J, Park J, Kim H and Lee B 2007 *Opt. Express* **15** 16596
[16] Wang B and Wang G P 2007 *Appl. Phys. Lett.* **90** 013114
[17] Moreno E, Rodrigo S G, Bozhevolnyi S I, Moreno L M and Vidal F J G 2008 *Phys. Rev. Lett.* **100** 023901
[18] Zhang H X, Gu Y and Gong Q H 2008 *Chin. Phys.* B **17** 2567
[19] Guo J and Adato R 2008 *Opt. Express* **16** 1232
[20] Arbel D and Orenstein M 2008 *Opt. Express* **16** 3114
[21] Boltasseva A, Volkov V S, Nielsen R B, Moreno E, Rodrigo S G and Bozhevolnyi S I 2008 *Opt. Express* **16** 5252
[22] Xue W R, Guo Y N, Li P and Zhang W M 2008 *Opt. Express* **16** 10710
[23] Xue W R, Guo Y N and Zhang W M 2009 *Chin. Phys.* B **18** 2529
[24] Guo Y N, Xue W R and Zhang W M 2009 *Acta Phys. Sin.* **58** 4168 (in Chinese)
[25] Dintinger J and Martin J F 2009 *Opt. Express* **17** 2364
[26] Zhu Z and Brown T G 2002 *Opt. Express* **10** 853
[27] Guo S P, Wu F, Albin S, Tai H and Rogowski R S 2004 *Opt. Express* **12** 3341
[28] Yu C P and Chang H C 2004 *Opt. Express* **12** 6165
[29] Johnson P B and Christy R W 1972 *Phys. Rev.* B **6** 4370
[30] Arnoldi W E 1951 *Quart. Appl. Math.* **9** 17